



# A Mathematical Study on Non-linear Boundary Value problem for Magnetohydrodynamic Fluid Flow

Manoharan Kalaivani, Vembu Ananthaswamy\*

Research Scholar, Research Centre and PG Department of Mathematics, The Madura College (Affiliated to Madurai Kamaraj University), Madurai, Tamil Nadu, India.

Research Centre and PG Department of Mathematics, The Madura College (Affiliated to Madurai Kamaraj University), Madurai, Tamil Nadu, India.

## KEYWORDS

Marangoni boundary layer flow;  
Permeable stretching surface;  
Magnetohydrodynamic (MHD);  
Non-Linear Boundary Value Problem; Modified q-Homotopy analysis method; Numerical solution;

**Abstract.** The influence of MHD upon the Marangoni boundary layer of hybrid nanofluid flow along an extended surface is mathematically analysed and presented in this work. Similarity transformations reduce the controlling equations to dimensionless form. The reduced simultaneous equations can be analytically resolved. The semi-analytical expressions for the dimensionless velocity as well as temperature are attained by utilizing Ananthaswamy Sivasankari technique (ASM) and Modified q-Homotopy analysis approach (Mq-HAM) respectively. The results of the dimensionless quantities for the amounts of physical components including dimensionless skin friction coefficient and non-dimensional Nusselt number are depicted in tabular and graphical forms to interpret significant consequences. The physical parameters involved in the model are depicted graphically to show their effects on the velocity and temperature respectively. The applied magnetic field parameter's direction and strength have a significant impact on the fluid flow. Our results on these parameters are used in fields where precise control of heat transfer and fluid flow is essential, such as crystal growth, microfluidics, welding processes, and the manufacturing of electronic components. The proposed technique shall be extended to address non-linear challenges in physical science especially MHD flow issues.

2024 Sharif University of Technology. All rights reserved.

## 1. Introduction

When compared to conventional fluid flow, scholars had a strong sense of motivation to assess the implications of nanofluid (NF) flow. In the wide range of scientific and engineering applications, boundary layer theory is indispensable. Engineering sciences typically deal with nonlinear problems, especially those involving heat transfers.

Abdullah et al.'s [1] computational study demonstrates how MHD influences the hybrid copper-aluminium oxide/water nanofluid flow on an extending surface in the Marangoni boundary layer, which enhances the efficiency of heat transmission. Punitha et al. [2] comprehensively mentioned the MHD NF's boundary layer flow and examined the impacts of certain physical elements influencing MHD NF flow. Devi and Devi [3] introduce an idea of hybrid nanofluid (HNF) in addition to an enhanced model of its thermophysical properties.

\*.Corresponding author.Tel: +918903550705  
E-mail address: [ananthaswamy@maduracollege.edu.in](mailto:ananthaswamy@maduracollege.edu.in)

### To cite this article:

M. Kalaivani, V. Ananthaswamy "A mathematical study on non-linear boundary value problem for Magnetohydrodynamic fluid flow", Scientia Iranica (20xx), xx(xx), pp.yyyy-yyyy  
<https://doi.org/10.24200/sci.2023.60676.6935>

Several academic studies were conducted to investigate nonlinear boundary value problems [4-10]. Ananthaswamy et al. [11] thoroughly analysed the MHD flow across an extending sheet. When heat radiation and a magnetic field are present, Aly and Ebaid [12] investigated the flow through the Marangoni boundary layer of HNF embedded in an opaque medium. They looked at how the field of velocity dropped as the volume fraction and magnetic field increased.

In order to meet industrial demands, HNF has been invented and is being investigated mathematically and it provides improved heat transfer capability. The two methods for creating HNF are mixing hybrid nanoparticles with the base fluid or spreading several kinds of nanoparticles at the base. Oil, ethylene glycol and water are examples of base fluids, whereas copper (Cu), silver (Ag), aluminium oxide ( $\text{Al}_2\text{O}_3$ ), titanium dioxide ( $\text{TiO}_2$ ) and copper oxide ( $\text{CuO}$ ) are the nanoparticle materials. The flow of thermal Marangoni convection was numerically analysed by Khashi'ie et al. [13] across an extending sheet and came to the conclusion that, in decreasing flows, heat transfer rate increased with a rising Cu volume percentage, and in stretching flows, with a Marangoni parameter. According to Sidik et al. [14], the HNF exhibits superior thermal conductivity in comparison to both base fluid and simple nanofluid.

There are several reviews of HNF on boundary layer flow from this literature to read further [15-18]. Ananthaswamy et al. [19] found a new analytical method called ASM to solve various boundary value problems. Sivasankari and Ananthaswamy [20] investigated the viscosity dissipation effect of motile microorganisms in the Darcy-Forchheimer NF via a non-linear extended sheet under analytical study. In [21 and 22], HAM is used in numerous and diverse applications.

The literature cited in this study motivates us to expand on Khashi'ie et al.'s [13] study, which exclusively examined the HNF without a magnetic field and discovered that the magnetic field variable causes the HNF of copper-aluminium oxide/water flows through a porous expandable surface in a Marangoni boundary layer flow.

Using Soret, Dufour, non-linear radiation, activation energy effects, and entropy generation analysis, S. C. Shiralashetti et al. [23] have employed a Legendre wavelet-based numerical method to solve the system of non-linear differential equations that arise in the study of a Marangoni convective flow of dusty Ree-Eyring fluid over a Riga plate in a Darcy-Forchheimer medium. In the study by Kumar.D et al., [24] the topic of nanofluid flow with radiation impact along a stretching sheet in a porous medium is covered. Additionally, a consistent magnetic field is applied. kerosene oil, the base fluid, and suspended particles of copper aluminium oxide ( $\text{Cu-Al}_2\text{O}_3$ ) combine to form the hybrid nanofluid, which takes into account the Marangoni boundary condition. Shafee Ahmad et al. [25] looked at the mathematical aspects of the energy transfer and entropy-generating processes through natural convection. The study is conducted in a square enclosure containing exothermic and endothermic blocks. Shafee Ahmad et al.'s [26] work employs the finite element approach to examine how isothermal sources and sinks affect natural convection and entropy formation for Casson fluids.

The Marangoni boundary layer flow problems have been numerically solved in previous literature, but responses relating to velocity, temperature, and other physical characteristics of importance are not expressed directly. By explicitly supplying the semi-analytical formulations for the governing equations, we bridge the gap by performing an analytical investigation on the Marangoni boundary layer flow.

The primary goal of this study is to ascertain how the control parameter affects the Marangoni boundary layer of hybrid nanofluid flow along an extended surface. Utilizing ASM and Mq-HAM, the semi-analytical expressions for velocity and temperature are explicitly given. The physical factors affecting the model are illustrated graphically. Moreover, the skin friction factor and Nusselt number are portrayed to show the influence of significant parameters involved in this model.

## 2. Mathematical formulation of the Problem

Investigations are conducted on a continuous 2-D MHD Marangoni hybrid nanofluid flow through a penetrable elongating sheet. Presumably, the particles of base fluids are in thermal equilibrium and also the fluid moves in an impermeable, laminar manner. Moreover, the application of the Cartesian coordinate system  $(x, y)$  is made (Figure 1).  $u_w(x) = ax$  where

$a > 0$  is the sheet's velocity and  $T_w(x) = T_\infty + T_0 \left( \frac{x}{L} \right)^2$  is sheet's

temperature, here  $T_\infty$ ,  $T_0$  and  $L$  are respectively the ambient, initial temperature and length. Additionally, a surface temperature difference that created surface tension ( $\sigma$ ) is the primary cause of flow induction. Devi and Devi [3] made the assumption that temperature has a linear effect on surface tension.

$$\sigma = \sigma_0 [1 - \gamma_T (T - T_\infty)], \gamma_T = - \frac{1}{\sigma_0} \frac{\partial \sigma}{\partial T} \quad (1)$$

Where  $\sigma_0$  denotes interface's surface tension,  $\gamma_T$  represents the coefficient of temperature tension at the surface and  $\sigma_0 > 0$ . Additionally, a uniform magnetic field  $B_0$  is utilized in the surface's normal direction.

According to Devi and Devi [3], the controlling equations of NF will be expressed in  $(x, y)$  coordinates as follows [1]: the primary focus of these equations is figuring out how the control parameter affects boundary layer separation.

$$u \frac{\partial u}{\partial x} + v \frac{\partial v}{\partial y} = 0 \quad (2)$$

$$u \frac{\partial u}{\partial x} + v \frac{\partial u}{\partial y} = \frac{\mu_{hnf}}{\rho_{hnf}} \frac{\partial^2 u}{\partial y^2} - \frac{\sigma_{hnf}}{\rho_{hnf}} B_0^2 u \quad (3)$$

$$u \frac{\partial T}{\partial x} + v \frac{\partial T}{\partial y} = \frac{k_{hnf}}{(\rho c_p)_{hnf}} \frac{\partial^2 T}{\partial y^2} \quad (4)$$

Subject to the bounding requirements

$$v = v_0 \mu_{hnf} \frac{\partial u}{\partial y} \bigg|_{y=0} = \lambda \frac{\partial \sigma}{\partial y} \bigg|_{y=0} = \lambda \frac{\partial T}{\partial y} \bigg|_{y=0},$$

$$T = T_w(x) \text{ at } y = 0, u \rightarrow 0, T \rightarrow T_\infty \text{ as } y \rightarrow \infty \quad (5)$$

Here  $u$  and  $v$  are respectively the velocity components in  $x$  and  $y$  directions, whereas  $T$ ,  $v_0$  and  $\lambda$  denotes temperature, constant mass flux velocity and constant parameter. Further,

$\mu_{hnf}$ ,  $\rho_{hnf}$ ,  $k_{hnf}$  and  $(\rho C_p)_{hnf}$  are the dynamic viscosity, density, thermal conductivity and heat capacity, whose expansion is provided in Table 1. The attributes of nanoparticles and water are described by the subscripts  $f$  and  $n$ . Table 2 lists the thermal and physical attributes of  $f$  and  $n$ .

We present the subsequent non-dimensional aspects to the similarity solutions [1] of eqns. (2) to (4), along with the corresponding boundary requirements in eqn. (5):

$$\left. \begin{aligned} u &= axf'(\xi), v = -\sqrt{av_f} f(\xi), \\ \theta(\xi) &= \frac{T - T_\infty}{T_w - T_\infty}, \xi = \frac{y}{\sqrt{\frac{v_f}{a}}} \end{aligned} \right\} \quad (6)$$

Here prime represents differentiation with respect to  $\xi$

Therefore,

$$v_0 = -\sqrt{av_f} S, \quad (7)$$

Here  $S$  refers to constant mass flux velocity.

Putting eqn. (6) in eqns. (3) and (4), the ODEs are [1],

$$\lambda_1 f'''' - M\lambda_3 f' + \lambda_2 (f f'' - f'^2) = 0 \quad (8)$$

$$\frac{1}{Pr} \frac{\lambda_4}{\lambda_5} \theta'' + f\theta' - 2f'\theta = 0 \quad (9)$$

$$\text{Here } \lambda_1 = \frac{\mu_{hnf}}{\mu_f}, \quad \lambda_2 = \frac{\rho_{hnf}}{\rho_f}, \quad \lambda_3 = \frac{\sigma_{hnf}}{\sigma_f}, \quad \lambda_4 = \frac{k_{hnf}}{k_f},$$

$$\lambda_5 = \frac{(\rho C_p)_{hnf}}{(\rho C_p)_f}, \quad Pr = \frac{(C_p \mu)_f}{k_f} \text{ represents the Prandtl}$$

number and  $M$  denotes the magnetic field parameter.

The dimensionless boundary requirements are [1]

$$\left. \begin{aligned} f(0) &= S, f''(0) = -2Ma\lambda(1 - \phi)^{2.5}(1 - t_2)^{2.5}, \\ f'(\xi) &\rightarrow 0 \text{ as } \xi \rightarrow \infty \end{aligned} \right\} \quad (10)$$

$$\theta(0) = 1 \text{ at } \xi = 0, \quad \theta(\xi) \rightarrow 0 \text{ as } \xi \rightarrow \infty \quad (11)$$

$$\text{Here } Ma = \frac{\sigma_0 \gamma_T T_0}{L^2 a \sqrt{a \rho_f \mu_f}} \text{ represents the Marangoni}$$

parameter and we say that  $S$  as suction and injection respectively, if  $S > 0$  and  $S < 0$ .

Furthermore, we define local Nusselt number  $Nu_x$  as:

$$Nu_x = \frac{xq_w}{k_f(T_w - T_\infty)}, \quad (12)$$

Here  $q_w$  refers to surface heat flux which is mentioned below:

$$q_w = -k_{hnf} \left( \frac{\partial T}{\partial y} \right)_{y=0} \quad (13)$$

Using eqn. (6), eqn. (12) and eqn. (13), we get

$$Re_x^{-\frac{1}{2}} Nu_x = \frac{k_{hnf}}{k_f} [-\theta'(0)], \quad (14)$$

$$\text{Here } Re_x = \frac{U_w(x)}{v_f} \text{ represents the local Reynolds number.}$$

### 3. Semi-Analytical Solution utilizing ASM and Modified q-Homotopy Analysis Method

The Ananthaswamy-Sivasankari method (ASM) is an

innovative approach to third-order ODE estimation [19, 20]. It is useful for solving each linear and non-linear DE. Numerous non-linear boundary requirement issues in the physical, chemical, and biological sciences, particularly MHD flow issues shall be readily addressed with this approach. Nonetheless, the new approach that has been proposed can be used to handle problems related to initial and boundary requirements. The approach is quite easy to comprehend and use. There are just three unknown constants in the solution, which depends on the differential equation order.

The Homotopy analysis approach, a potent analytical technique to sort out non-linear situations, was introduced by Liao [27–30]. An analytical outcome in terms of an infinite power series is offered by this method. Nevertheless, evaluating this response and deriving numerical values from the infinite power series are practically required. For the purpose of verifying whether the Homotopy Analysis Technique (HAM) outcome with limited-term is valid, the system of DEs was resolved. In contrast to other methods of perturbation, the homotopy analysis approach is a useful instrument. Using the auxiliary parameter in the homotopy analysis approach, we have an easy way to regulate and alter the convergence zone of the solution series.

Mq-HAM is a powerful tool for tackling non-linear differential equations regarding boundary layer problems. On comparing to the numerical method, it provides an approximate solution with explicit form and it doesn't require any step size at any stage. The calculation procedure is simple and easy to understand. On comparing to other analytical methods, the results attained by this method are more accurate and faster convergence.

The subsequent semi-analytical expression depicts the velocity, temperature, skin friction as well as Nusselt number in non-dimensional form by employing Modified q-Homotopy analysis methodology (Mq-HAM).

#### 3.1. Semi-Analytical result of Velocity profile utilizing ASM

The velocity profile's solution to eqn. (8) is as follows:

$$f(\xi) = l + me^{a\xi} + ne^{-a\xi} \quad (15)$$

$$f'(\xi) = ame^{a\xi} - ane^{-a\xi} \quad (16)$$

Putting the eqn. in (10) in eqn. (8), we have  $l, m$  and  $n$  as:

$$l = S - \frac{A}{a^2}, \quad m = 0 \text{ and } n = \frac{A}{a^2} \quad (17)$$

Thus, the eqn. (15) becomes

$$f = S - \frac{A}{a^2} + \frac{A}{a^2} e^{-a\xi} \quad (18)$$

Now, by applying eqn. (18) in eqn. (10) and simplifying,

$$\begin{aligned} & -a\lambda_1 A e^{-a\xi} + \frac{M\lambda_3 A e^{-a\xi}}{a} \\ & + \lambda_2 \left[ \left( S - \frac{A}{a^2} + \frac{A}{a^2} e^{-a\xi} \right) A e^{-a\xi} - \frac{A^2}{a^2} e^{-2a\xi} \right] = 0 \end{aligned} \quad (19)$$

Now, by taking  $\xi = 0$ , the eqn. (19) becomes,

$$-a\lambda_1 A + \left( \frac{M\lambda_3 A}{a} \right) + \lambda_2 \left( SA - \frac{A^2}{a^2} \right) = 0 \quad (20)$$

By solving the above eqn. (20), we shall have the value of  $a$  and on further simplification the approximate analytical solution of eqn. (8) can be found as follows:

$$f = S - \frac{A}{a^2} + \frac{A}{a^2} e^{-a\xi} \quad (21)$$

### 3.2. Approximate analytical solution of the temperature profile utilizing Modified q-Homotopy Analysis Method (Mq-HAM)

After substituting the eqn. (21) in eqn. (9), we get the following reduced temperature profile equation

$$\frac{1}{\text{Pr}} \frac{\lambda_4}{\lambda_5} \theta'' + \left( S - \frac{A}{a^2} + \frac{A}{a^2} e^{-a\xi} \right) \theta' - 2 \left( \frac{-A}{a} e^{-a\xi} \right) \theta = 0 \quad (22)$$

The Homotopy for eqn. (22) is as follows:

$$(1-np) \left( \frac{1}{\text{Pr}} \frac{\lambda_4}{\lambda_5} \theta'' \right) = hp \left( \frac{1}{\text{Pr}} \frac{\lambda_4}{\lambda_5} \theta'' + \left( S - \frac{A}{a^2} + \frac{A}{a^2} e^{-a\xi} \right) \theta' - 2 \left( \frac{-A}{a} e^{-a\xi} \right) \theta \right) \quad (23)$$

Where  $h \in [-1, 1]$  and  $n \geq 1$ .

The initial approximation for the above eqn. (23) is given by  $\theta_0(0) = 1, \theta_0(\infty) \rightarrow 0$  (24)

$\theta_i(0) = 0, \theta_i(\infty) \rightarrow 0, i \in \mathbb{N}$  (25)

The approximate analytical solution for the eqn. (22) is

$$\theta = \theta_0 + p\theta_1 + p^2\theta_2 + \dots \quad (26)$$

Substituting the eqn. (25) in eqn. (23), and equating the powers of  $p$ 's coefficient,

$$p^0 : \frac{1}{\text{Pr}} \frac{\lambda_4}{\lambda_5} \theta_0'' = 0 \quad (27)$$

$$p^1 : \frac{1}{\text{Pr}} \frac{\lambda_4}{\lambda_5} (\theta_1'' - n\theta_0'') = h \left( \frac{1}{\text{Pr}} \frac{\lambda_4}{\lambda_5} \theta_0'' + \left( S - \frac{A}{a^2} + \frac{A}{a^2} e^{-a\xi} \right) \theta_0' - 2 \left( \frac{-A}{a} e^{-a\xi} \right) \theta_0 \right) \quad (28)$$

By utilizing Mq-HAM, the initial guessing solution for  $p^0$ , we get

$$\theta_0 = e^{-c_1\xi}, \quad (29)$$

Where

$$c_1 = 2 \frac{\lambda_4}{(k_f k_{bf})(0.1)\text{Pr}} \quad (30)$$

On solving  $p^1$  and utilizing the bounding conditions of  $\theta_i(0)$ , we get

$$\theta_1 = \frac{1}{n} (C + B_1 e^{-c_1\xi} + B_2 e^{-(a+c_1)\xi}), \quad (31)$$

Where,

$$C = -1 - \frac{\text{Pr} \lambda_5 h}{\lambda_4} \left[ \frac{1}{c_1} \left( \frac{\lambda_4 c_1}{\text{Pr} \lambda_5} - S + \frac{A}{a^2} \right) + \frac{2aA - c_1 A}{a^2 (a + c_1)^2} \right] \quad (32)$$

$$B_1 = 1 + \frac{\text{Pr} \lambda_5 h}{c_1 \lambda_4} \left( \frac{\lambda_4 c_1}{\text{Pr} \lambda_5} - S + \frac{A}{a^2} \right) \text{ and} \quad (33)$$

$$B_2 = \frac{\text{Pr} \lambda_5 h}{\lambda_4} \left( \frac{2aA - c_1 A}{a^2 (a + c_1)^2} \right) \quad (34)$$

By Mq-HAM approach, we get

$$\theta = \lim_{p \rightarrow 1} \theta_0 + p\theta_1 = \theta_0 + \theta_1 \quad (35)$$

Hence, the semi-analytical solution to eqn. (9) is obtained by putting the eqn. (29) and eqn. (31) in the eqn. (35), we have

$$\theta(\xi) = e^{-c_1\xi} + \frac{1}{n} (C + B_1 e^{-c_1\xi} + B_2 e^{-(a+c_1)\xi}), \quad (36)$$

Where  $C, B_1, B_2$  were defined in eqn. (32) to eqn. (34).

## 4. Results and Discussion

This part constitutes the analysis of different physical components in these nanofluid flow models. Additionally, a comparison of the analytical solution that was depicted in eqn. (21) of the dimensionless velocity profile and eqn. (36) of the dimensionless temperature profile along with the numerical results described in [1] was included. Figure 1 illustrates the physical structure of the nanofluid challenge. The estimation of analytical and numerical results to velocity and temperature in non-dimensional form with various physical parameter values including magnetic parameter  $M$ , Marangoni parameter  $Ma$ , Prandtl number  $\text{Pr}$ , a constant parameter  $\lambda$ , aluminum oxide ( $\text{Al}_2\text{O}_3$ ) volume fraction  $\phi_1$ , Copper (Cu) volume fraction  $\phi_2$  and the constant mass flux velocity  $S$  with  $S > 0$  for suction and  $S < 0$  for injection is shown in Figure 2 to 11. Figures 2 to 5 illustrate dimensionless velocity by considering the similarity variable.

From Figure 2, we can see that for various amounts of  $M$  and a few amounts of parameters  $\text{Pr}, \phi_1, \phi_2, Ma, S, \lambda$ , where the ASM and the previous work results are totally coincident, the dimensionless velocity  $f'(\xi)$  falls as the similarity variable  $\xi$  increases. Moreover, if the magnetic field parameter increases, then the corresponding induced Lorentz force will also get increased. Thus, the Marangoni effect is most noticeable and the most notable velocity reduction occurs close to the fluid surface.

Figure 3 exhibits how the copper volume fraction  $\phi_2$  affects the fluid flow velocity profile for numerous values of  $\phi_2$  and some specified values of  $\text{Pr}, \phi_1, Ma, M, S, \lambda$ , the corresponding dimensionless velocity  $f'(\xi)$  falls as  $\xi$  grows. As the similarity variable  $\xi$  grows, the velocity profile  $f'(\xi)$  diminishes, as revealed in Figure 4 for a range of constant mass flux velocity values  $S$  as well as for a few set of values of  $\text{Pr}, \phi_1, \phi_2, Ma, M, \lambda$ . Figure 5 shows how the fluid flow's velocity profile is affected by the Aluminium Oxide volume fraction  $\phi_1$ . The matching dimensionless velocity  $f'(\xi)$  decreases as  $\xi$  grows for a range of values of  $\phi_1$  and few constant values of  $\text{Pr}, \phi_2, Ma, M, S, \lambda$ . Figure 6 indicates the relationship between the growth of the velocity profile  $f'(\xi)$



and the similarity variable  $\xi$  for a range of Marangoni variables  $Ma$  and a few amounts of  $Pr, \phi_1, \phi_2, M, S, \lambda$ .

Figures 7 to 9 illustrate dimensionless temperature  $\theta(\xi)$  in relation to the similarity variable  $\xi$ . From Figure 7, we inferred that, when  $\theta(\xi)$  increases as the similarity variable  $\xi$  grows, for a small selection of amounts of the magnetic field variable  $M$  and a few amounts of  $Pr, \phi_1, \phi_2, Ma, S, \lambda$ . The induced Lorentz force in the boundary layer grew as the magnetic parameter rose. As a result, an increase in the Lorentz force decreases fluid motion and inhibits fluid flow. Thus, the temperature rises. For a range of constant mass flux velocity  $S$  values as well as for a few amounts of  $Pr, \phi_1, \phi_2, Ma, M, \lambda$ , Figure 8 demonstrates that the dimensionless temperature  $\theta(\xi)$  falls as the similarity variable  $\xi$  rises. The consequence of copper volume fraction  $\phi_2$  over the temperature curve is portrayed in Figure 9. Under a few set of constant values of the remaining parameters  $Pr, \phi_1, Ma, M, S, \lambda$  and an increased range of values of  $\phi_2$ , the corresponding dimensionless temperature  $\theta(\xi)$  increases as  $\xi$  grows. The  $h$ -curve for the third approximation is shown in Figure 10 for fixed parameter values of  $Pr, \phi_1, \phi_2, Ma, M, S, \lambda$ .

Figure 11 exhibits that the coefficient of skin friction  $C_f$  grows along with the constant parameter  $\lambda$  for some fixed amounts of  $Pr, S, Ma, M$  and by changing the values of  $\phi_1$ . With certain fixed values of  $Pr, \phi_1, \phi_2, S, M$  and by varying the values of  $Ma$ , Figure 12 displays how the coefficient of skin friction increases with the constant parameter. Higher the Marangoni parameter and volume fraction of aluminium oxide can further affect the skin friction factor because, depending on the particular flow configuration, surface tension-driven flow might increase shear stress. Figure 13 infers the Local Nusselt number  $Nu_x$  grows along  $\lambda$  regarding a few set of amounts of  $Pr, \phi_2, S, Ma, M$  and by changing the values of  $\phi_1$ . Based on the values of  $Ma$  and a few set of amounts of  $Pr, \phi_1, \phi_2, S, M$ , Figure 14 suggests that the Local Nusselt number grows with  $\lambda$ . By varying the values of  $Pr$  and with relation to a few set of amounts of  $\phi_1, \phi_2, S, Ma, M$ , Figure 15 implies that the Local Nusselt number grows. The main component affecting the local nusselt number, which indicates the relative strength of convection caused by surface tension. Greater local nusselt number is correlated with higher  $Ma$ ,  $Pr$  and  $\phi_1$ .

Table 3 clearly depicts the numerical and analytical outcomes of the skin friction coefficient for a few amounts of  $\phi_2$  as well as fixed values of the parameter  $Pr, \phi_1, S, Ma, M, \lambda$ , where  $n \geq 1$ . Table 4 investigates the numerical and analytical findings of  $Nu_x$  of certain amounts of  $\phi_2$  and specified quantities of the parameters  $Pr, \phi_1, S, Ma, M, \lambda$ , where  $n \geq 1$ . Table 5 gives the contrast of numerical as well as analytical outcomes of Local Nusselt number defined in eqn. (14) for numerous amounts of the parameters  $S$  and  $M$ , when  $n \geq 1$ ,  $Pr = 6.2, Ma = 1, \lambda = 1, \phi_1 = 0.1$  and  $\phi_2 = 0.09$ .

## 5. Conclusion

The impact of several physical characteristics of a nanofluid that passes over an extended surface with MHD was investigated in the current study. The controlling ODEs were resolved analytically by utilizing the Modified q-Homotopy analysis approach. When contrasted against the numerical findings, graphical results demonstrate an excellent fit. From the research, the following outcomes were particularly noteworthy:

- When the magnetic field parameter  $M$  increases and  $S < 0$ , the Local Nusselt number drops and concurrently, it rises at  $S > 0$ .
- The temperature rises and the velocity drops; when the magnetic field variable  $M$  and Cu volume fraction rises.
- The temperature and velocity drop when the suction parameter raises, alternatively the profiles of both rise when injection parameter increases.

These research findings will be helpful to researchers in the field of engineering and material sciences for analyzing the heat transfer rate and flow significance.

In future, we have to extend this method for solving boundary layer issues having highly non-linear differential equations governing the boundary layer, MHD flow with nanofluids and hybrid nanofluids.

## Acknowledgment

The Authors are thankful to Sri. S. Natanagopal, Secretary, The Madura College Board, Dr. J. Suresh, The Principal, The Madura College and Dr. C. Thangapandi, Head of the Department of Mathematics, The Madura College, Madurai, Tamil Nadu, India for their constant support to our research work.

## Funding Statement

This research did not receive any specific grant from funding agencies in the public, commercial, or not-for-profit sectors.

## Conflicts of Interest

The author declares that there is no conflict of interest regarding the publication of this article.

## References

- Abdullah, N.N., Som, A.N.M., Arifin, N.M. et al. "The Effect of MHD on Marangoni Boundary Layer of Hybrid Nanofluid Flow Past a Permeable Stretching Surface", *CFD Letters*, **15**(5), pp.65-73 (2023).  
<https://doi.org/10.37934/cfdl.15.5.6573>
- Punitha, S., Ananthaswamy, V. and Santhi, V.K. "Approximate Analytical Expression for the Influence of Flow of MHD Nanofluids on Heat and Mass Transfer", *CFD Letters*, **15**(11), pp.48-66 (2023).  
<https://doi.org/10.37934/cfdl.15.11.4866>
- Devi, S.A. and Devi, S.S.U. "Numerical investigation of hydromagnetic hybrid Cu-Al<sub>2</sub>O<sub>3</sub>/water nanofluid flow over a permeable stretching sheet with suction", *International Journal of Nonlinear Sciences and Numerical*

- Simulation*, **17**(5), pp.249-257 (2016).  
<https://doi.org/10.1515/ijnsns-2016-0037>
4. Ali, F.M., Nazar, R., Arifin, N.M. et al. "Unsteady shrinking sheet with mass transfer in a rotating fluid", *International Journal for Numerical Methods in Fluids*, **66**(11), pp.1465-1474 (2011).  
<https://doi.org/10.1002/flid.2325>
5. Shen, M., Wang, F. and Chen, H. "MHD mixed convection slip flow near a stagnation-point on a nonlinearly vertical stretching sheet", *Boundary value problems*, 2015, pp.1-15 (2015).  
<https://doi.org/10.1186/s13661-015-0340-6>
6. Najib, N., Bachok, N., Arifin, N.M. et al. "Stability analysis of stagnation-point flow in a nanofluid over a stretching/shrinking sheet with second-order slip, sores and dufour effects: A revised model", *Applied Sciences*, **8**(4), p.642 (2018).  
<https://doi.org/10.3390/app8040642>
7. Mahat, R., Saqib, M., Ulah, I., et al. "MHD Mixed Convection of Viscoelastic Nanofluid Flow due to Constant Heat Flux", *Journal of Advanced Research in Numerical Heat Transfer*, **9**(1), pp.19-25 (2022).  
<https://doi.org/10.37934/cfdl.14.9.5259>
8. Nadeem, S., Khan, M.R. and Khan, A.U. "MHD stagnation point flow of viscous nanofluid over a curved surface", *Physica Scripta*, **94**(11), p.115207 (2019).  
<http://dx.doi.org/10.1088/1402-4896/ab1eb6>
9. Ghosh, S. and Mukhopadhyay, S. "Stability analysis for model-based study of nanofluid flow over an exponentially shrinking permeable sheet in presence of slip", *Neural Computing and Applications*, **32**(11), pp.7201-7211 (2020).  
<https://doi.org/10.1007/s00521-019-04221-w>
10. Khan, A.A., Zaimi, K., Sufahani, S.F. et al. "MHD flow and heat transfer of double stratified micropolar fluid over a vertical permeable shrinking/stretching sheet with chemical reaction and heat source", *Journal of Advanced Research in Applied Sciences and Engineering Technology*, **21**(1), pp.1-14 (2020).  
<https://doi.org/10.37934/araset.21.1.114>
11. Ananthaswamy, V., Subanya, R.R. and Sivasankari, S. "A mathematical study on a steady MHD flow in double stratification medium", *CFD Letters*, **15**(10), pp.34-51 (2023).  
<https://doi.org/10.37934/cfdl.15.10.3451>
12. Aly, E.H. and Ebaid, A. "MHD Marangoni boundary layer problem for hybrid nanofluids with thermal radiation", *International Journal of Numerical Methods for Heat & Fluid Flow*, **31**(3), pp.897-913 (2021).  
<https://doi.org/10.1108/HFF-05-2020-0245>
13. Khashi'ie, N.S., Arifin, N.M., Pop, I., et al. "Thermal Marangoni flow past a permeable stretching/shrinking sheet in a hybrid Cu-Al", *Sains Malaysiana*, **49**(1), pp.211-222 (2020).  
<http://dx.doi.org/10.17576/jsm-2020-4901-25>
14. Sidik, N.A.C., Adamu, I.M., Jamil, et al. "Recent progress on hybrid nanofluids in heat transfer applications: a comprehensive review", *International communications in heat and mass Transfer*, **78**, pp.68-79 (2016).  
<https://doi.org/10.1016/j.icheatmasstransfer.2016.08.019>
15. Kumar, T.P. "Heat transfer of SWCNT-MWCNT based hybrid nanofluid boundary layer flow with modified thermal conductivity model", *Journal of Advanced Research in Fluid Mechanics and Thermal Sciences*, **92**(2), pp.13-24 (2022).  
<https://doi.org/10.37934/arfmts.92.2.1324>
16. Alsaedi, A., Muhammad, K. and Hayat, T. "Numerical study of MHD hybrid nanofluid flow between two coaxial cylinders", *Alexandria Engineering Journal*, **61**(11), pp.8355-8362 (2022).  
<https://doi.org/10.1016/j.aej.2022.01.067>
17. Wahid, N.S., Arifin, N.M., Khashi'ie, N.S., et al. "Flow and heat transfer of hybrid nanofluid induced by an exponentially stretching/shrinking curved surface", *Case Studies in Thermal Engineering*, **25**, p.100982 (2021).  
<https://doi.org/10.1016/j.csite.2021.100982>
18. Khashi'ie, N.S., Hafidzuddin, E.H., Arifin, N.M. et al. "Stagnation point flow of hybrid nanofluid over a permeable vertical stretching/shrinking cylinder with thermal stratification effect", *CFD Letters*, **12**(2), pp.80-94 (2020).  
<https://www.akademiarbaru.com/submit/index.php/cfdl/article/view/3217>
19. Ananthaswamy, V., Sivasankari, S. and Sivasundaram, S. "A new approximate analytical method (ASM) for solving some non-linear boundary value problems", *Mathematics in Engineering, Science & Aerospace (MESA)*, **15**(1) (2024).  
<https://nonlinearstudies.com/index.php/mesa/article/view/3455>
20. Sivasankari, S. and Ananthaswamy, V. "A mathematical study on non-linear ordinary differential equation for Magnetohydrodynamic flow of the Darcy-Forchheimer nanofluid", *Computational Methods for Differential Equations*, **11**(4), pp.696-715 (2023).  
DOI: [10.22034/cmde.2023.55330.2302](https://doi.org/10.22034/cmde.2023.55330.2302)
21. Ananthaswamy, V., Nithya, T. and Santhi, V.K.. "Mathematical analysis of the Navier-stokes equations for steady Magnetohydrodynamic flow", *Journal of Information and Computational Science*, **10**, pp.989-1003 (2020).  
DOI: [10.12733/JICS.2020.V10I3.535569.12014](https://doi.org/10.12733/JICS.2020.V10I3.535569.12014)
22. Chitra, J., Ananthaswamy, V., Sivasankari, S. et al. "A new approximate analytical method (ASM) for solving non-linear boundary value problem in heat transfer through porous fin", *Mathematics in Engineering, Science & Aerospace (MESA)*, **14**(1) (2023).  
<https://nonlinearstudies.com/index.php/mesa/article/view/3058>
23. Shiralashetti, S.C., Kulkarni, P.I. and Hanaji, S.I. "Legendre wavelet based numerical method for the solution of marangoni convective flow of dusty ree-erying fluid over a riga plate with activation energy". *J.Umm Al-Qura Univ. Appl. Sci.* (2024). <https://doi.org/10.1007/s43994-024-00202-5>
24. Kumar, D., Agrawal, P., Dadheech, P.K. et al. "Numerical study of Marangoni convective hybrid-nanofluids flow over a permeable stretching surface." *International Journal of*

- Thermofluids* 23 (2024): 100750.  
<https://doi.org/10.1016/j.ijft.2024.100750>
25. Ahmad, Shafee, Dong Liu, et al. "MHD double diffusive flow analysis in a permeable cavity: An endothermic versus exothermic based study." *International Communications in Heat and Mass Transfer* 162 (2025): 108604.  
<https://doi.org/10.1016/j.icheatmasstransfer.2025.108604>
  26. Ahmad, Shafee, Bai Mbye Cham, Dong Liu, et al. "Numerical analysis of heat and mass transfer of MHD natural convection flow in a cavity with effects of source and sink." *Case Studies in Thermal Engineering* 53 (2024): 103926.  
<https://doi.org/10.1016/j.icheatmasstransfer.2025.108604>
  27. Liao, S.J. "An approximate solution technique not depending on small parameters: a special example", *International Journal of Non-Linear Mechanics*, **30**(3), pp.371-380 (1995).  
[https://doi.org/10.1016/0020-7462\(94\)00054-E](https://doi.org/10.1016/0020-7462(94)00054-E)
  28. Liao, S.J. "A kind of approximate solution technique which does not depend upon small parameters—II. An application in fluid mechanics", *International Journal of Non-Linear Mechanics*, **32**(5), pp.815-822 (1997).  
[https://doi.org/10.1016/S0020-7462\(96\)00101-1](https://doi.org/10.1016/S0020-7462(96)00101-1)
  29. Liao, S.J. "An explicit, totally analytic approximate solution for Blasius' viscous flow problems", *International Journal of Non-Linear Mechanics*, **34**(4), pp.759-778 (1999).  
[https://doi.org/10.1016/S0020-7462\(98\)00056-0](https://doi.org/10.1016/S0020-7462(98)00056-0)
  30. Liao, S.J. "A uniformly valid analytic solution of two-dimensional viscous flow over a semi-infinite flat plate", *Journal of Fluid Mechanics*, **385**, pp.101-128 (1999).  
<https://doi.org/10.1017/S0022112099004292>

**Figure 1.** Schematic Diagram of the model

**Figure 2.**  $f'(\xi)$  with  $\xi$  for a set of values of  $Pr, \phi_1, \phi_2, Ma, S$  and  $\lambda$  by varying the values of  $M$ .

**Figure 3.**  $f'(\xi)$  with  $\xi$  for specified amounts of  $Pr, \phi_1, S, Ma, M$  and  $\lambda$  by differing the amounts of  $\phi_2$ .

**Figure 4.**  $f'(\xi)$  with similarity variable  $\xi$  for some fixed values of  $Pr, \phi_1, \phi_2, Ma, M$  and  $\lambda$  by varying the values of  $S$

**Figure 5.** The non-dimensional velocity with  $\xi$  for some specified amounts of  $Pr, \phi_2, S, Ma, M$  and  $\lambda$  by varying the values of  $\phi_1$ .

**Figure 6.** The non-dimensional velocity with  $\xi$  for some specified amounts of  $Pr, \phi_1, \phi_2, S, Ma$  and  $\lambda$  by varying the values of  $Ma$ .

**Figure 7.** The dimensionless temperature with the similarity variable for some fixed amounts of  $Pr, \phi_1, \phi_2, S, Ma$  and  $\lambda$  by varying the values of  $M$ .

**Figure 8.** The non-dimensional temperature with similarity variable for some fixed values of  $Pr, \phi_1, \phi_2, Ma, M$  and  $\lambda$  by varying  $S$ .

**Figure 9.** The non-dimensional temperature with similarity variable by varying the values of  $\phi_2$  for some fixed amounts of  $Pr, \phi_1, S, Ma, M$  and  $\lambda$ .

**Figure 10.**  $h$  curve for the dimensionless temperature for some fixed parameters

**Figure 11.**  $C_f$  against  $\lambda$  for some fixed amounts of  $Pr, \phi_2, S, Ma$  and  $M$  by varying the values of  $\phi_1$

**Figure 12.**  $C_f$  against  $\lambda$  for some fixed amounts of  $Pr, \phi_1, \phi_2, S$  and  $M$  by varying the values of  $Ma$ .

**Figure 13.**  $Nu_x$  against  $\lambda$  by varying a few values of  $\phi_1$ , for a specified amounts of  $Pr, \phi_2, S, Ma, M$ .

**Figure 14.**  $Nu_x$  against  $\lambda$  by varying a few values of  $Ma$  and a specified amounts of  $Pr, \phi_1, \phi_2, S, M$ .

**Figure 15.**  $Nu_x$  against  $\lambda$  by varying a few values of  $Pr$  and a specified amounts of  $\phi_1, \phi_2, S, Ma, M$ .

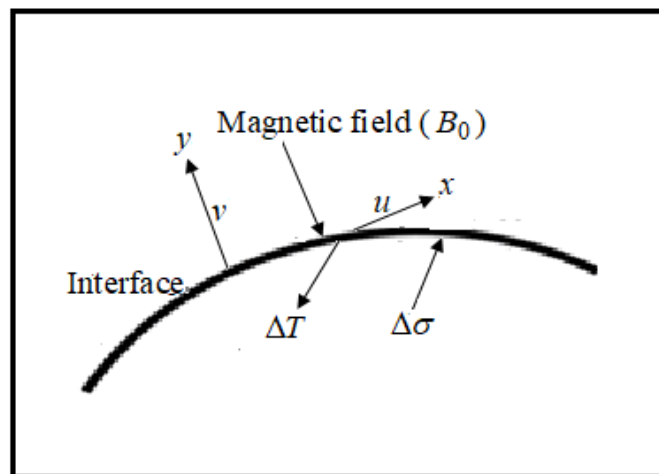


Figure 1.



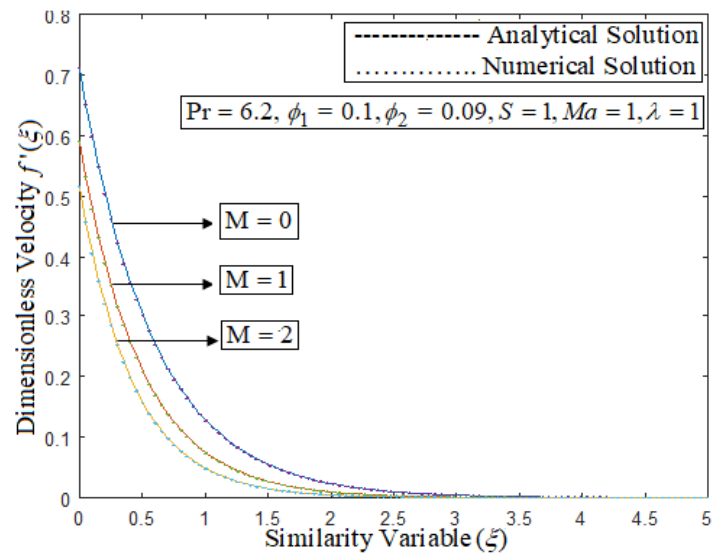


Figure 2.

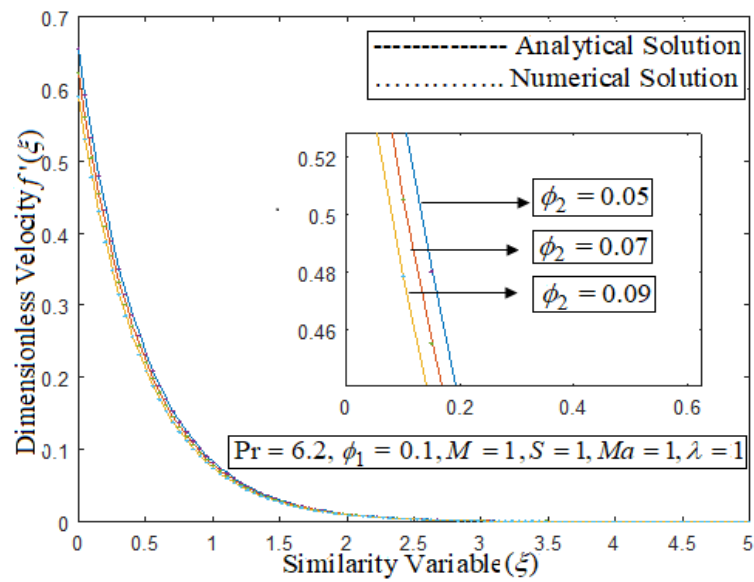


Figure 3.

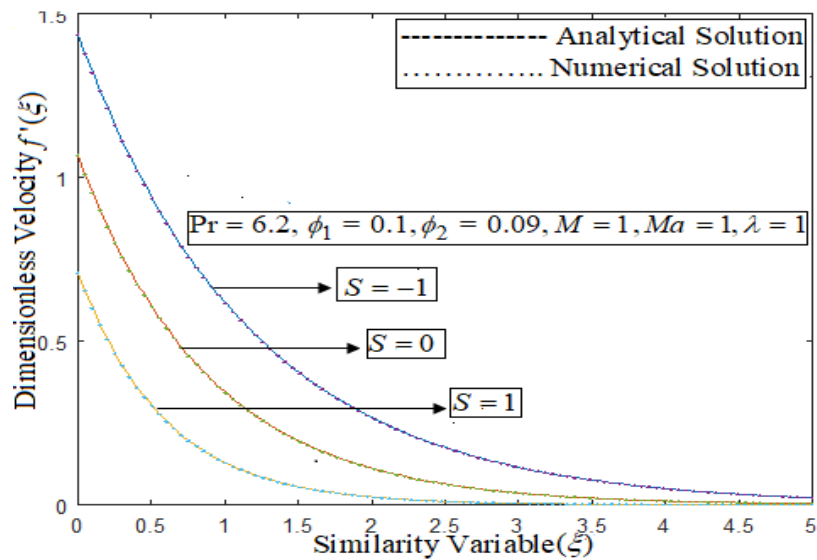


Figure 4.

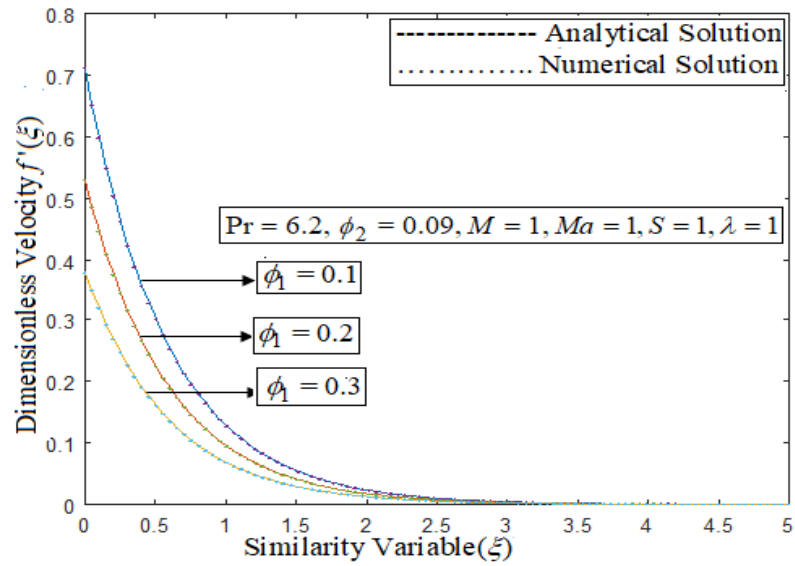


Figure 5.

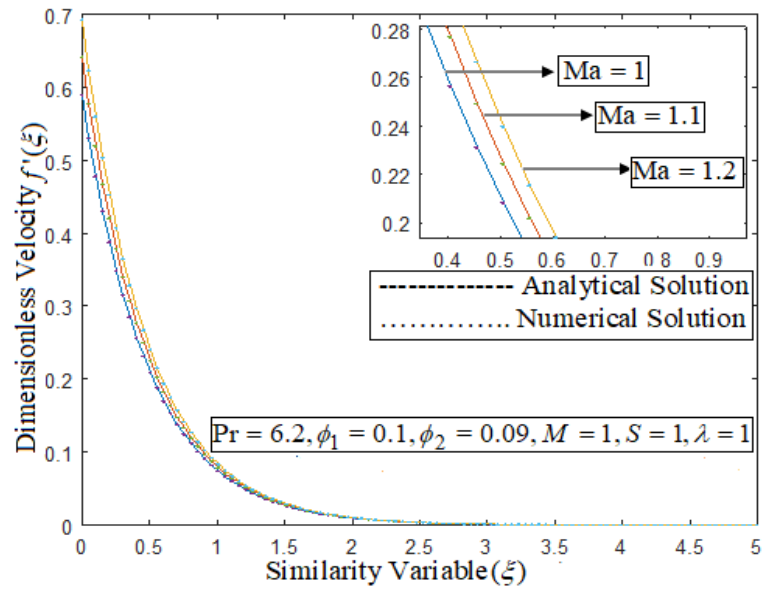


Figure 6.

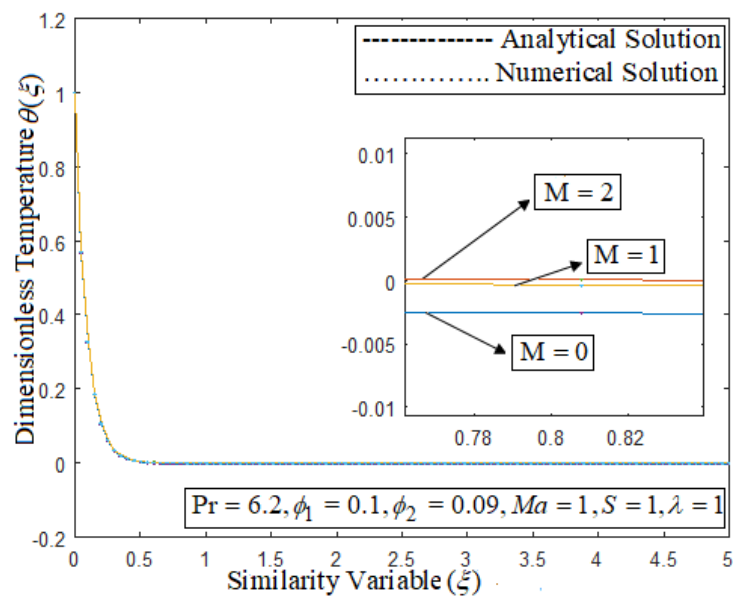


Figure 7.

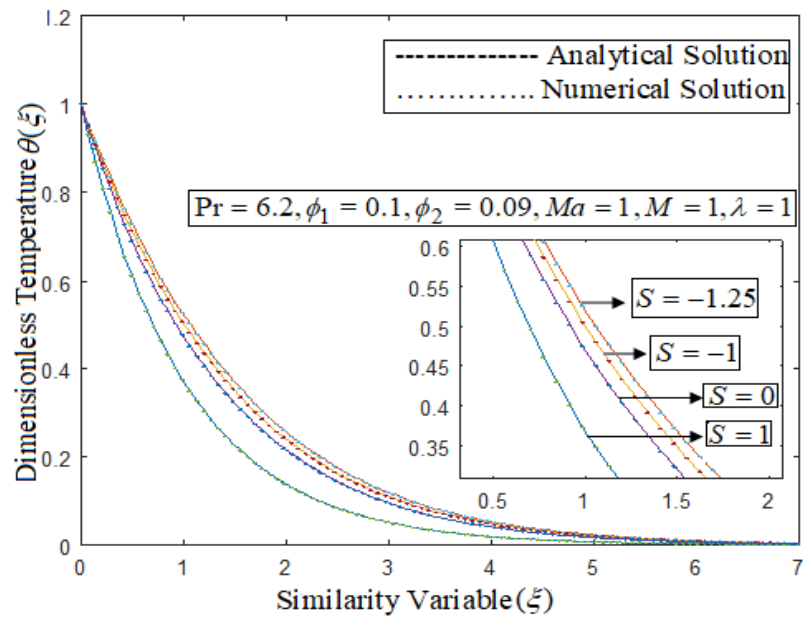


Figure 8.

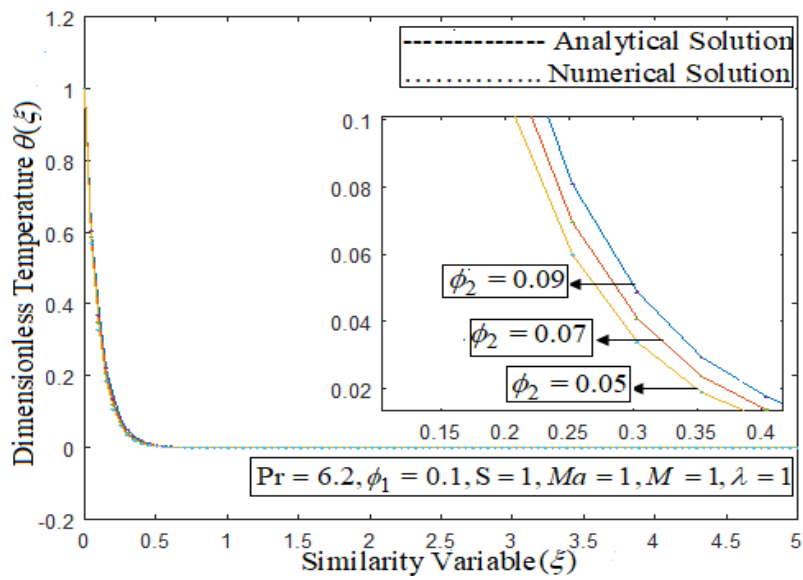


Figure 9.

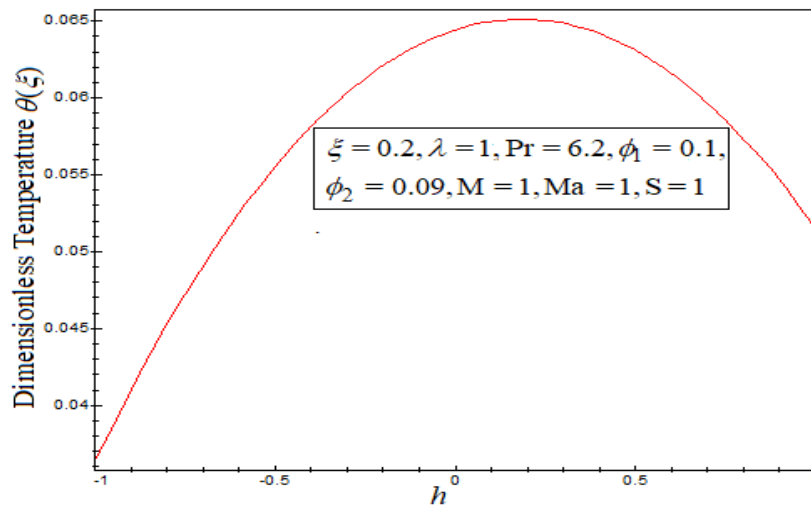


Figure 10.

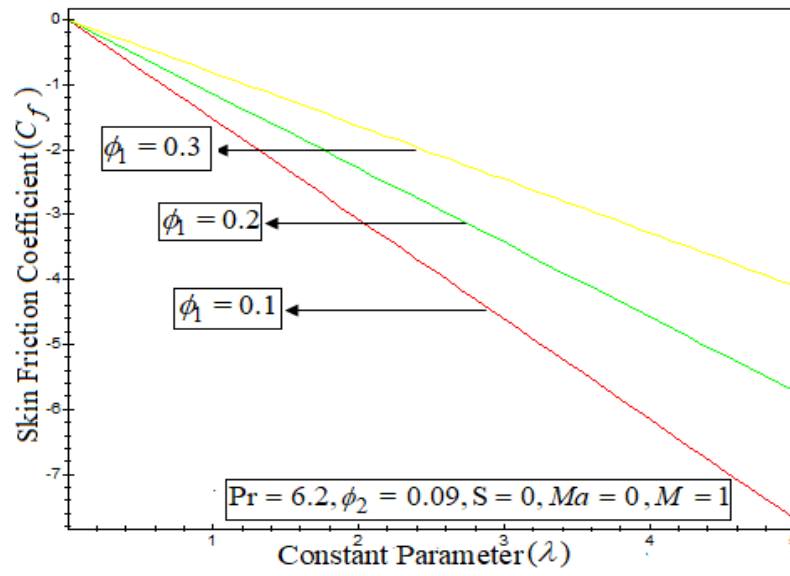


Figure 11.

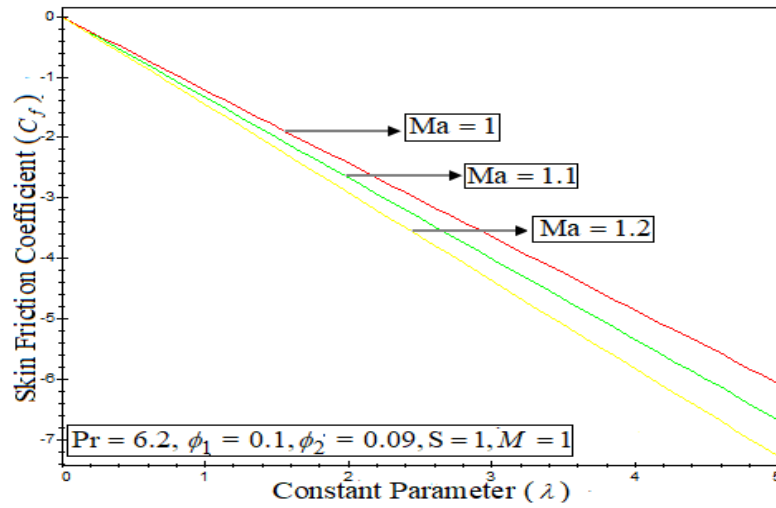


Figure 12.

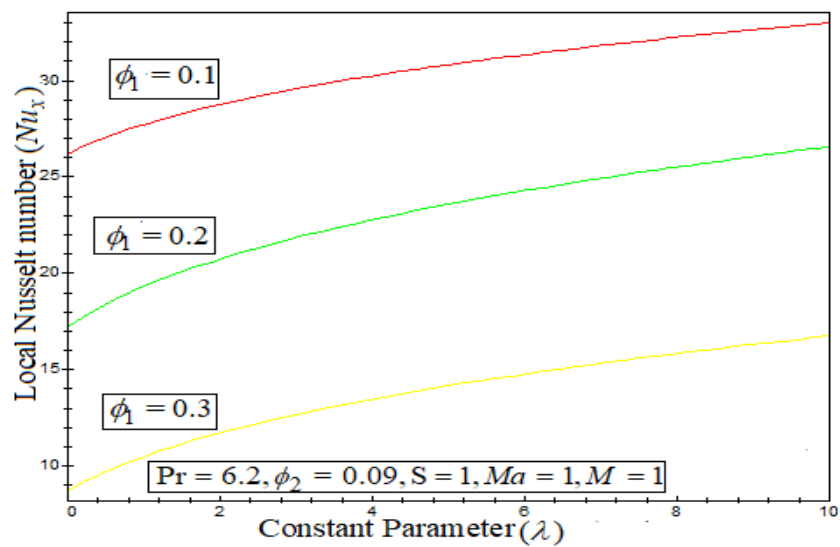


Figure 13.

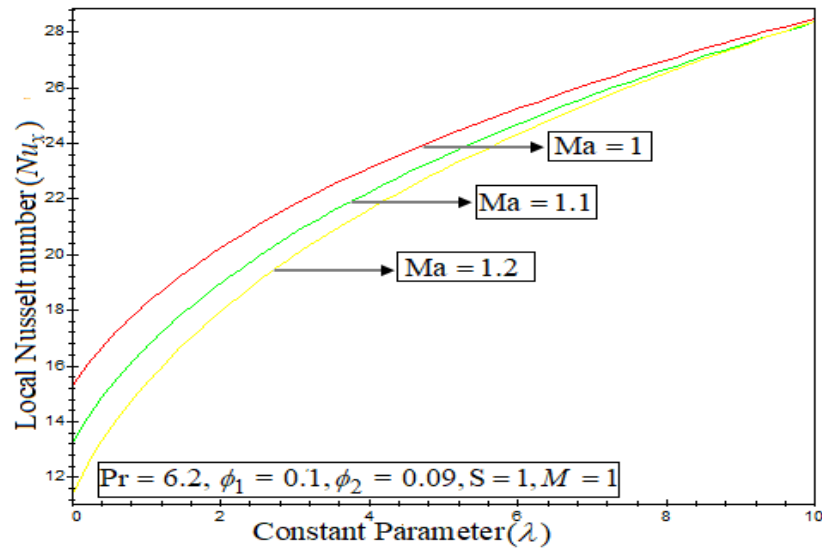


Figure 14.

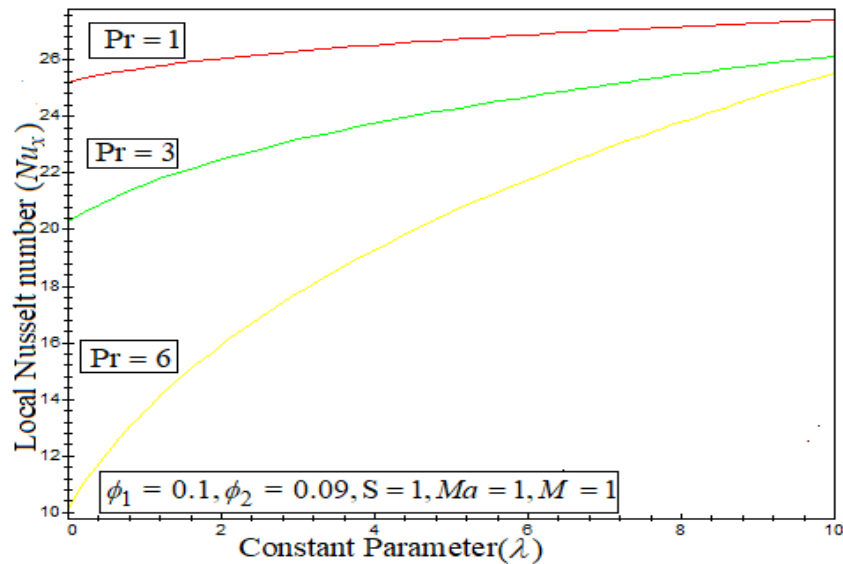


Figure 15.

## TABLES WITH CAPTIONS

**Table 1.** The physical attributes of NF and HNF (Khashi'ie et al.,[13])

**Table 2.** Water and nanoparticles's thermo physical attributes (Devi and Devi [3])

**Table 3.** Comparison of numerical and analytical solutions to the coefficient of Skin Friction for Cu-water with  $Ma=1, M=0, \lambda=1, S=0$  and  $\phi_1=0$ .

**Table 4.** Comparison of numerical and analytical outcomes to Local Nusselt number of Cu-water with  $Ma=1, M=0, \lambda=1, S=0$  and  $\phi_1=0$ .

**Table 5.** Comparison of numerical and analytical outcomes to the Local Nusselt number defined in eqn. (14) for numerous amounts of the parameters  $S$  and  $M$ , when  $Pr=6.2, Ma=1, \lambda=1, \phi_1=0.1$  and  $\phi_2=0.09$



**Table 1.**

Properties	Hybrid Nanofluid
Heat Capacity	$(\rho C_p)_{hnf} = (1 - \phi_2)[(1 - \phi_1)(\rho C_p)_f + \phi_1(\rho C_p)_{s1}] + \phi_2(\rho C_p)_{s2}$
Dynamic Viscosity	$\frac{\mu_{hnf}}{\mu_f} = \frac{1}{(1 - \phi_1)^{2.5}(1 - \phi_2)^{2.5}}$
Density	$\rho_{hnf} = (1 - \phi_2)[(1 - \phi_1)\rho_f + \phi_1\rho_{s1}] + \phi_2\rho_{s2}$
Electrical Conductivity	$\frac{\sigma_{hnf}}{\sigma_{bf}} = \left[ \frac{\sigma_{s2} + 2\sigma_{bf} - 2\phi_2(\sigma_{bf} - \sigma_{s2})}{\sigma_{s2} + 2\sigma_{bf} + \phi_2(\sigma_{bf} - \sigma_{s2})} \right]$ ,where $\frac{\sigma_{hnf}}{\sigma_f} = \left[ \frac{\sigma_{s1} + 2\sigma_f - 2\phi_1(\sigma_f - \sigma_{s1})}{\sigma_{s1} + 2\sigma_f + \phi_1(\sigma_f - \sigma_{s1})} \right]$
Thermal Conductivity	$\frac{k_{hnf}}{k_{bf}} = \left[ \frac{k_{s2} + 2k_{bf} - 2\phi_2(k_{bf} - k_{s2})}{k_{s2} + 2k_{bf} + \phi_2(k_{bf} - k_{s2})} \right]$ ,where $\frac{k_{bf}}{k_f} = \left[ \frac{k_{s1} + 2k_f - 2\phi_1(k_f - k_{s1})}{k_{s1} + 2k_f + \phi_1(k_f - k_{s1})} \right]$

**Table 2.**

Physical Characteristics	$Al_2O_3(s_1)$	$Cu(s_2)$	Water ( $f$ )
$\rho(kg/m^3)$	3970	8933	997.1
$C_p(J/kgK)$	765	385	4179
$k(W/mK)$	40	400	0.6130
$\sigma(s/m)$	$35 \times 10^6$	$59.6 \times 10^6$	$5.5 \times 10^{-6}$

**Table 3.**

$\phi_2$	Khashi'ie et al.[13]	Abdullah et al.[1]	Current work
0.1	-1.53687	-1.53687	-1.53687
0.2	-1.14487	-1.14487	-1.14487

**Table 4.**

$\phi_2$	Khashi'ie et al.[13]	Abdullah et al.[1]	Current work
0.1	-3.40694	-3.40680	-3.40560
0.2	-2.58874	-2.58854	-2.58514

**Table 5.**

$S$	$M$	Abdullah et al.[1]	Current work
-0.5	0	3.429572	3.427499
	1	2.789934	2.788807
	2	2.308835	2.309254
0	0	4.374033	4.373702
	1	3.73552	3.735923
	2	3.265533	3.265379
0.5	0	5.778110	5.777692

1	5.279899	5.279428
2	4.942785	4.942151

## Nomenclature

Symbol	Meaning
$u, v$	Component in the $x, y$ direction
$T_\infty$	Ambient fluid
$T_w$	Sheet's temperature
$T_0$	Characteristic temperature
$\sigma$	Surface tension
$B_0$	Uniform magnetic field
$T$	Temperature
$\mu_{hnf}$	Dynamic Viscosity
$\lambda$	Constant parameter
$\rho_{hnf}$	Density
$S$	Constant mass flux velocity
$k_{hnf}$	Thermal Conductivity
$(\rho C_p)_{hnf}$	Heat capacity
$\xi$	Similarity variable
$C_f$	Coefficient of skin friction
$M$	Magnetic field parameter
$f'(\xi)$	Dimensionless velocity
$Ma$	Marangoni parameter
$Nu_x$	Local Nusselt number
$\theta(\xi)$	Dimensionless temperature
$Re_x$	Local Reynolds number
$\phi_1$	Aluminum oxide ( $Al_2O_3$ ) volume fraction
$\phi_2$	Copper (Cu) volume fraction
Subscripts	
$f$	Fluid (water)
$nf$	Nanofluid
$bf$	Basefluid
$hnf$	Hybrid nanofluid

## BIOGRAPHY

### Author-1: Mrs. M. Kalaivani

Mrs. M. Kalaivani is an accomplished academic in the field of mathematics with a strong foundation in both teaching and research. She completed her M.Sc. in Mathematics from The Madura College (Autonomous), Madurai, Tamil Nadu, in 2015. Her academic journey continued with the completion of an M.Phil. in Mathematics from the same institution in 2016, further solidifying her expertise in the subject. Currently, she is pursuing a Ph.D. under the co-guidance of Dr. V. Ananthaswamy, an Associate Professor of Mathematics at The Madura College.

With over six years of teaching experience across both Engineering and Arts Colleges, Mrs. Kalaivani has honed her skills in imparting complex mathematical concepts to students. Her research interests focus on solving non-linear differential equations through asymptotic methods, a critical area in mathematical analysis. She has actively participated in various National and International Conferences, presenting her research findings and contributing to the broader academic community. Her commitment to mathematics, both in teaching and research, reflects her dedication to advancing the field.

### Author-2: Dr. V. Ananthaswamy (Corresponding author)

Dr. V. Ananthaswamy is a distinguished mathematician with over two decades of teaching experience and a significant research portfolio. He began his academic journey with an M.Sc. in Mathematics from The Madura College (Autonomous), Madurai, Tamil Nadu, in 2000, followed by an M.Phil. in Mathematics from Madurai Kamaraj University in 2002. He furthered his academic pursuits by earning a Ph.D. from Madurai Kamaraj University in 2013, under the guidance of Dr. L. Rajendran.

With 25 years of experience teaching in Engineering Colleges, Arts Colleges, and Deemed Universities, Dr. Ananthaswamy has built a reputation as an expert in his field. His research interests are centered on mathematical modeling, particularly using differential equations and asymptotic approximations. He also focuses on the analysis of non-linear reaction diffusion equations across various scientific disciplines, including physics, chemistry, and biology.

Dr. Ananthaswamy has published more than 165 peer-reviewed articles in both National and International Journals and has completed a minor research project funded by the University Grants Commission (UGC). He is currently an Associate Professor of Mathematics at The Madura College (Autonomous), where he continues to inspire students and contribute to the advancement of mathematical research.

## CONTACT DETAILS

### 1. Author 1

Name: M. Kalaivani

Full Name: Manoharan Kalaivani

Phone: +91 9080623740

Email: kalaimano462@gmail.com

Affiliation: Research Scholar (Part Time), Research Centre and PG Department of Mathematics, The Madura College (Affiliated to Madurai Kamaraj University), Madurai, Tamil Nadu, India

### 2. Author 2 (Corresponding author)

Name: V. Ananthaswamy

Full Name: Vembu Ananthaswamy

Phone: +91 8903550705

Email: ananthaswamy@maduracollege.edu.in

Affiliation: Associate Professor, Research Centre and PG Department of Mathematics, The Madura College (Affiliated to Madurai Kamaraj University), Madurai, Tamil Nadu, India